RSC Advances

PAPER

View Article Online
View Journal | View Issue



Cite this: *RSC Adv.*, 2025, **15**, 49918

# Plasmonic filter paper for microplastic detection: SERS enhancement, size dependence, and quantitative limitations

Minjeong Kim, Donggeon Lee, Dong-Wook Shin, Sangyeob Lee, Choong-Heui Chung and Jung-Sub Wi *

The public concern over microplastic exposure in daily life has increased the demand for reliable detection methods. Surface-Enhanced Raman Scattering (SERS), a candidate method for microplastic analysis, enables chemical identification of microplastics at trace levels. This study evaluated the dependence of SERS on microplastic size and its inherent limitations in quantitative analysis. SERS-active substrates were fabricated by coating a gold film onto a conventional filter paper using oblique-angle deposition. The signal-enhancement effect of the SERS-active substrate was evaluated using electromagnetic simulations and experimental measurements of polystyrene microplastics. For 1 μm polystyrene microplastics, Raman signals were detectable even without SERS enhancement, indicating that plasmonic amplification is not essential for microplastics larger than a few micrometers. Meanwhile, 200 nm polystyrene particles require SERS for signal detection. Across both particle sizes, no definitive correlation was observed between the Raman signal intensity and particle concentration within the range of 10–1000 ppm. This highlights a limitation of SERS analysis for microplastic detection due to the fact that the sizes of the analytes are comparable to the size of the laser focal spot. Our findings demonstrate that using SERS to quantify microplastic concentrations without large-scale data analysis techniques, such as area mapping, can lead to misleading interpretations.

Received 1st October 2025
Accepted 8th December 2025

DOI: 10.1039/d5ra07464a

rsc.li/rsc-advances



## Introduction

With the increasing prevalence of plastics, microplastics—defined as particles ranging in size from less than 5 mm down to the nanometer scale—have become widely distributed not only in the environment but also within the human body.[1–3] These microplastics increase the levels of reactive oxygen species, induce cytotoxic and inflammatory responses, and cause DNA damage in human cells.[3–5] Moreover, because of their large surface area, microplastics function as vectors for adsorbing and delivering hazardous chemicals, raising significant concerns about their adverse influence on human health.[6,7] Consequently, a variety of analytical methodologies, including microscopy, spectroscopy, and mass spectrometry, have been extensively investigated for the detection and identification of microplastics.[8–10] Raman spectroscopy—particularly surface-enhanced Raman scattering (SERS)—holds considerable potential owing to its ability to provide molecular-specific chemical identification and enhance signal intensities through plasmonic nanostructures, enabling analysis of small sample volumes.[11–20] Recent research has demonstrated the efficacy of SERS in identifying diverse microplastics such as polystyrene, polyethylene, and polypropylene within complex environmental matrices, with detection limits reported at parts-per-million (ppm) concentrations.[21–26] Despite extensive research on the application of SERS sensors to microplastics, critical challenges and limitations related to quantitative assessment—specifically factors influencing the relationship between microplastic concentration and Raman signal intensity—have been insufficiently addressed. In this study, we propose a plasmonic filter paper that can be used as both an SERS-active substrate and a conventional filter. By employing this plasmonic filter paper to measure polystyrene particles with sizes of 1 μm and 200 nm, we provide definitive experimental evidence supporting the applicability of SERS for microplastic detection while also elucidating potential limitations inherent to this approach.

## Experimental

### Fabrication of plasmonic filter papers

Plasmonic filter papers were fabricated by depositing a 40 nm-thick gold film on commercial filter paper (HM.5301055, Hyundai Micro, Korea). Prior to Au deposition, 1 nm-thick titanium was deposited on the filter paper as an adhesion promoting layer. Both titanium and gold depositions were carried out using a thermal evaporator (DaON 1000 TE, DAON

*Department of Materials Science and Engineering, Hanbat National University, Daejeon, Republic of Korea. E-mail: jungsub.wi@hanbat.ac.kr*

Co., Korea) at a base pressure of $2 \times 10^{-6}$ torr with a deposition rate of 0.1 nm $s^{-1}$.

### Measurements of SERS spectra

Monodispersed polystyrene particles with diameters of 200 nm and 1 μm (3200A and 4100A, ThermoFisher Scientific, USA) were employed as microplastic models at a concentration of 1 wt% in an aqueous solution. These suspensions were diluted with deionized water to achieve the target concentrations. Subsequently, 2 mL aliquots were filtered through filter paper housed within a membrane filter holder (PP-25, Advantec, Japan). The filter papers were utilized either in their pristine form or after the deposition of a gold film. After filtration, the Raman spectra of the microplastics retained on the filter papers were acquired using a Raman microscope (NS220, Nanoscope Systems, Korea) with an excitation laser wavelength of 633 nm. Spectral acquisition was performed using a 100× objective lens with an integration time of 3 s/measurement.

### Electromagnetic simulation

The spatial distribution of the squared local electric field amplitude on the surface of the gold-coated filter paper was computed using three-dimensional finite-difference time-domain (FDTD) simulation software (ANSYS Lumerical FDTD). Given that the refractive index of cellulose is reported to be approximately 1.5 within the visible spectrum, this value was adopted for the filter substrate.[27,28] The dielectric constants for gold were sourced from the Johnson and Christy dataset, which was integrated within the FDTD software.

## Results and discussion

### Characterization of gold-coated filter papers

To assess the applicability and constraints of SERS for microplastic detection, SERS-active substrates were fabricated by thermally evaporating gold onto filter paper. During Au deposition, the filter paper was continuously rotated, with the Au flux incident either perpendicularly or at an oblique angle of 55° relative to the filter paper surface, as shown in Fig. 1(a) and (b). Oblique-angle deposition was employed to achieve a conformal coating on the fibrous and rough surfaces of the filter paper. Scanning electron microscopy (SEM) images (Fig. 1(c)) revealed a pronounced shadowing effect in the case of normal-incidence deposition, indicating incomplete Au coverage. Conversely, oblique-angle deposition resulted in a nanostructured Au thin film that conformally coated the entire surface, as shown in Fig. 1(d). Because of these morphological distinctions, subsequent experiments utilized Au-coated filter papers prepared by oblique-angle deposition.

The SEM image in Fig. 2(a) shows a magnified view of the nanostructured Au film on the filter paper. The granular Au film naturally forms nanoscale gaps between the Au networks, which are expected to enhance the local electric fields and thereby amplify the Raman signals. Three-dimensional FDTD simulations were conducted to investigate the electromagnetic properties of this nanostructure. The contrast-enhanced SEM image in Fig. 2(a) was extended to a depth of 40 nm along the *z*-axis and imported as a nanostructured Au film for the simulation. A plane wave with a wavelength of 630 nm was used as the incident light source. Fig. 2(b) and (c) show the squared magnitudes

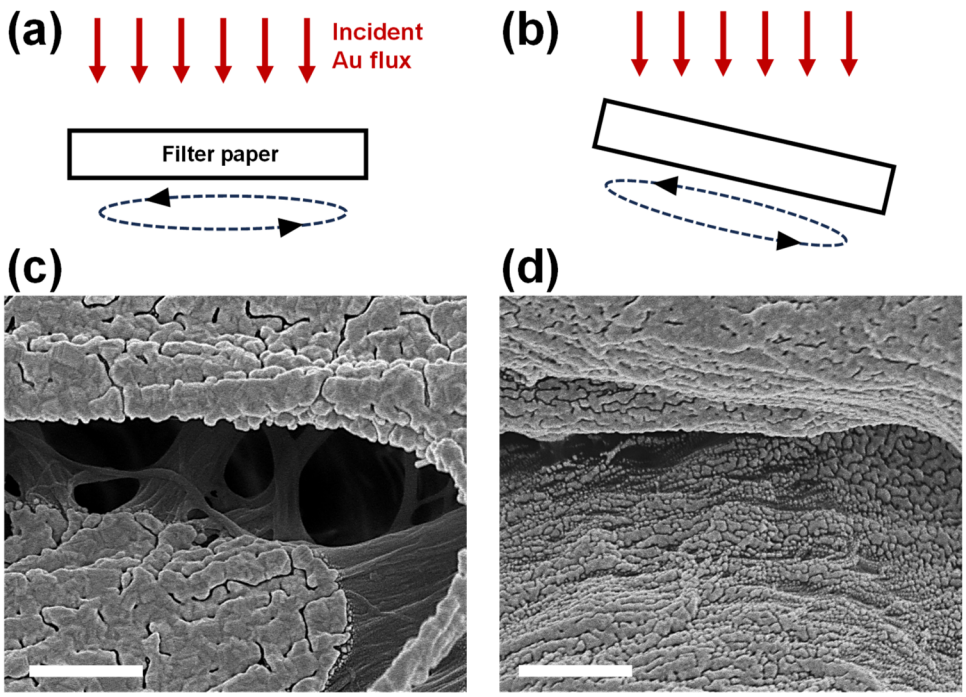


Fig. 1 Fabrication of Au-coated filter paper. (a and b) Schematic of the Au evaporation step. The incident direction of the Au flux was (a) perpendicular and (b) inclined at an angle of 55° relative to the surface of the filter paper. In both cases, the filter papers were rotated during the Au deposition. (c and d) SEM images of the Au-coated filter papers on which Au was deposited (c) perpendicularly and (d) at an inclined angle to the surface. All scale bars represent 500 nm.

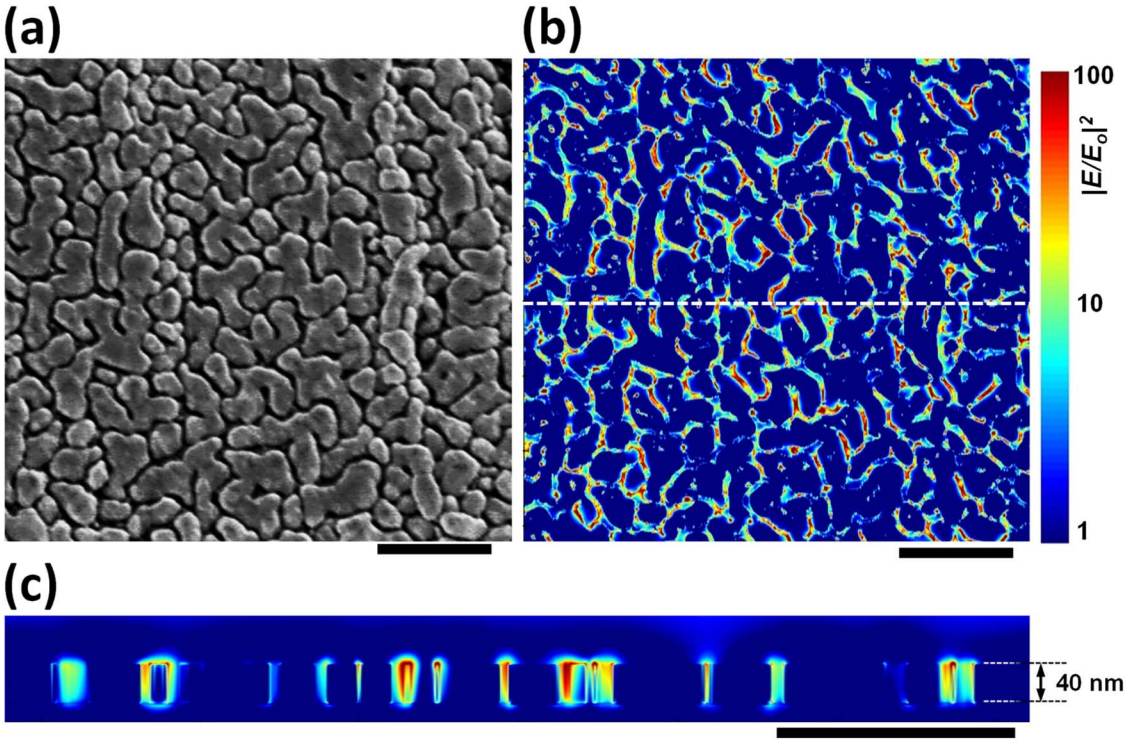


Fig. 2 Plasmonic characteristics of Au-coated filter paper. (a) SEM image and (b and c) squared magnitude of the local electric field amplitude of the Au film on filter paper. For the three-dimensional FDTD simulation, the planar image in (a) was elongated to 40 nm in the *z*-direction and imported as the nanostructured Au film. The wavelength of the incident light was 630 nm. The electric field was monitored at (b) the surface of the Au film and (c) the cross-section indicated by the dotted line in (b). All scale bars represent 300 nm.

of the local electric fields at the surface and cross-sectional planes of the Au-coated filter paper, respectively. The electric field-enhanced regions, highlighted in red and yellow in Fig. 2(b), are distributed throughout the simulation domain and correspond closely to the nanoscale gaps observed in the SEM image. These results indicate that the Au-coated filter paper effectively enhances the local electric fields and can potentially serve as an SERS substrate. However, as shown in Fig. 2(c), the vertical range of the enhanced fields is limited to approximately 10 nm or less from the Au surface, raising concerns about its usefulness for microplastic detection, although not for small molecule detection.

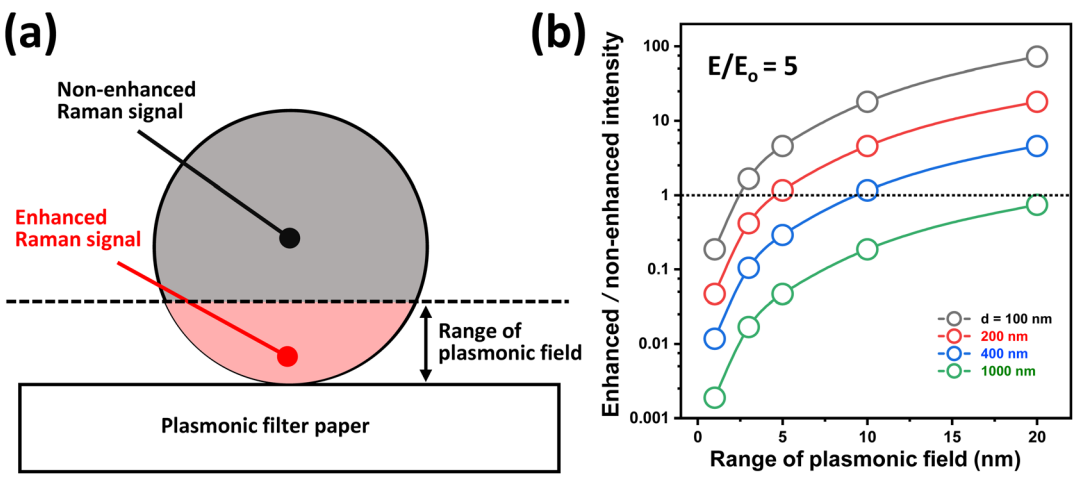


Fig. 3 Influence of microplastic size on SERS analysis. (a) Schematic illustrating the penetration of the plasmonic field from the surface of the plasmonic filter paper to the base of the microplastic particle. The regions at the bottom of the microplastics, where Raman signal enhancement is anticipated, are highlighted in red. (b) Ratio of enhanced to non-enhanced Raman signal intensities calculated for a single microplastic with diameters ranging from 100 nm to 1 μm. It was assumed that the amplitude of the enhanced electric field is five times the initial value, and this enhanced field is laterally uniform across the plasmonic filter paper. The vertical extent of the enhanced field varied between 1 nm and 20 nm from the surface of the plasmonic paper.

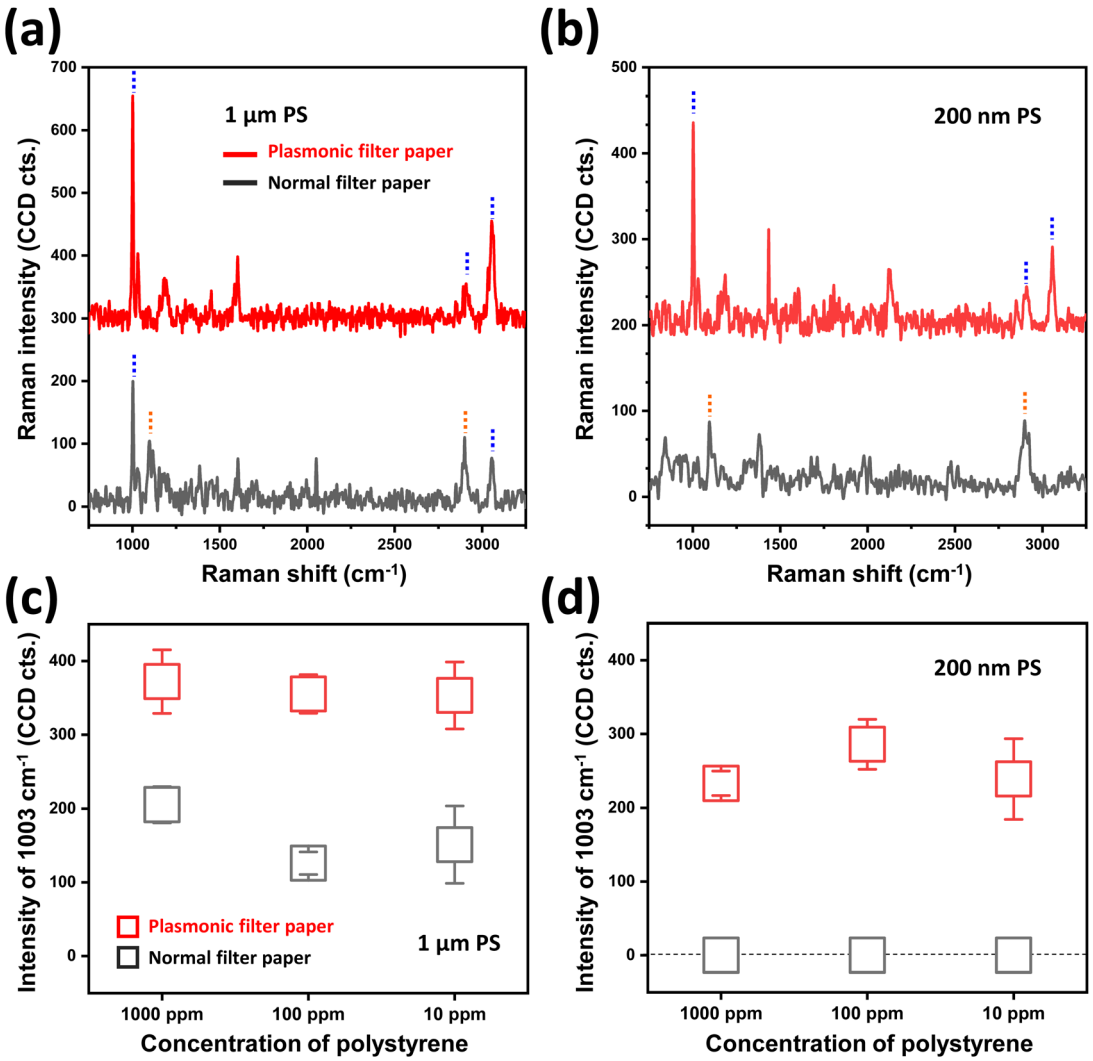


Fig. 4 Detection sensitivity of polystyrene microplastic. (a and b) Raman spectra obtained from plasmonic (depicted in red) and normal filter paper (depicted in black) after filtering a polystyrene microplastics colloidal solution with a concentration of 1000 ppm. (c and d) Average intensities of the Raman peaks of polystyrene at 1003 $cm^{-1}$, measured at three distinct concentrations (10, 100, and 1000 ppm) on plasmonic (red) and normal filter paper (black). The diameters of the polystyrene microplastics correspond to 1 μm in panels (a) and (c) and 200 nm in panels (b) and (d), respectively.

### Modeling of SERS signal dependence on microplastic size

To consider the usefulness of the fabricated plasmonic filter paper for microplastic detection, we modeled the interaction between the microplastics and the plasmonic field, where the enhanced electric fields extended vertically from the filter paper surface and reached the bottom part of an overlying microplastic particle, as illustrated in Fig. 3(a). To simplify the model, the enhanced electric field was assumed to exist solely within the vertical range indicated by the side arrows in Fig. 3(a) and to be uniform in magnitude. Consequently, only the portion of the microplastics within this enhanced field region (depicted in red) contributed to the SERS signal. The SERS signal intensity was thus proportional to the volume of this red region multiplied by the fourth power of the enhancement factor ($|E/E_0|^4$). Based on the simulation results shown in Fig. 2, the enhanced field ratio ($|E/E_0|$) was set to 5 within the enhanced field region. The intensity of the unamplified Raman signal was considered proportional to the microplastic volume above the dashed line in Fig. 3(a), with an enhancement factor of unity ($|E/E_0|^4 = 1$) outside the enhanced field. Fig. 3(b) presents the calculated ratios of SERS to unamplified Raman signal intensities for single microplastic particles with diameters ranging from 100 nm to 1 μm. The vertical range of the enhanced field varied from 1 to 20 nm. As the microplastic size decreased, the microplastic volume fraction within the enhanced field region increased, thereby augmenting the relative contribution of the SERS signal. For instance, with a 10 nm enhanced field range, microplastics smaller than 400 nm exhibited SERS signal intensities surpassing those of the unamplified Raman signals. Conversely, for 1 μm particles, the SERS signal remained weaker than the unamplified Raman signal, even though the enhanced field extended up to 20 nm from the surface. These findings suggest that under the modeled conditions, the proposed SERS sensor is advantageous primarily for detecting nanoplastics

smaller than 400 nm but is unnecessary for microplastics exceeding 1 μm in size.

### Validation of detection sensitivity and quantification limit

Finally, we experimentally assessed the applicability and limitations of SERS for microplastic detection. A polystyrene microplastic colloidal solution with a concentration of 1000 ppm was filtered through either plasmonic or normal filter paper. Fig. 4(a) and (b) show representative Raman spectra measured after filtering the microplastic solution, with sizes of (a) 1 μm and (b) 200 nm. For 1 μm particles, the Raman signals were readily detectable without plasmonic enhancement. Characteristic Raman peaks at 1003, 1030, 2915, and 3060 $cm^{-1}$ were observed for both plasmonic and normal filter papers, as indicated by the blue dotted lines in Fig. 4(a).[29] Although the normal filter paper exhibited cellulose Raman peaks at 1098 and 2897 $cm^{-1}$ (orange dotted lines),[30] and the polystyrene signal intensity was lower than that of the plasmonic filter, microplastic detection was successful across concentrations of 1000 to 10 ppm (Fig. 4(c)). This indicates that SERS is not essential for detecting micrometer-sized particles with a sufficient volume. By contrast, Raman signals for 200 nm polystyrene particles were only detectable using the plasmonic substrate (Fig. 4(b)), which is consistent with the model results in Fig. 3 that predict the increased importance of plasmonic enhancement for smaller particles. Determining the particle size at which plasmonic enhancement becomes necessary requires careful consideration of several factors, including the Raman scattering cross-section of the material and the detection sensitivity of the spectrometer. Nevertheless, if it is restricted to the polystyrene used in this study and the specifications of our spectrometer (noise level of approximately 30 CCD counts), an estimation can be made. Considering that the Raman signal from 1 μm particles measured on normal filter paper and that the intensity of the unamplified Raman signal scales with particle volume, it can be inferred that plasmonic signal enhancement would become essential for detecting particles whose volume is less than half that of 1 μm particles.

Despite the demonstrated utility of the plasmonic filter paper, no correlation was observed between Raman signal intensity and concentration for 200 nm polystyrenes (Fig. 4(d)) or for 1 μm particles (Fig. 4(c)). This underscores the limitations of point analysis in Raman spectroscopy, where the signal intensities are averaged over multiple measurement points. When measuring a Raman signal at a specific point on a sample, the signal is expected to be proportional to the amount of analytes present at that point. Unlike in molecular analysis, in microplastic analysis, the analyte size is comparable to the laser focal volume. Consequently, there would be little change of the Raman signal in spot analysis of microplastic, except in cases where the size of the plastic is quite small compared to the laser spot, resulting in a sufficient change in the number of microplastics within the spot. The lack of correlation between analyte concentration and Raman signal intensity is expected to remain the same for microplastics with sizes intermediate between 200 nm and 1 μm, as well as for microplastics larger than 1 μm. Therefore, quantitative microplastic analysis *via* SERS necessitates statistical approaches involving large-area mapping,[24,31] as well as preprocessing steps, such as size classification of microplastics.[32] Additionally, the development of SERS sensors with surfaces flatter than that of the current plasmonic filter paper is required to maintain consistent laser focal planes during large-area mapping.

## Conclusions

In this study, we propose a plasmonic filter paper that enables the enhancement of the Raman signal and filtering of microplastics. Electromagnetic field simulations and experimental Raman measurements demonstrated that SERS provides significant signal amplification for the detection of nanoscale particles. However, SERS is not necessary for microplastics larger than several micrometers in size. Furthermore, it was demonstrated that point-based SERS measurements are insufficient for correlating the detected signal intensity with the microplastic concentration. These findings elucidate both the potential and limitations of SERS for microplastic detection and provide considerations for appropriate microplastic SERS sensors, such as size-based classification and large-area mapping.

## Author contributions

Minjeong Kim: conceptualization, methodology, investigation, validation, and writing – original draft. Donggeon Lee: methodology and investigation. Dong-Wook Shin: conceptualization, writing, and review. Sangyeob Lee: data curation, resources, and validation. Choong-Heui Chung: data curation, resources, and validation. Jung-Sub Wi: conceptualization, resources, supervision, writing, review, and editing.

## Conflicts of interest

There are no conflicts to declare.

## Data availability

All the data necessary to support the conclusions of this study are provided in the manuscript. Additional information is available from the corresponding author on request.

## Acknowledgements

This research was supported by the 2025 Hanbat National University Academic and Cultural Research Foundation.

## References

1 J. P. G. L. Frias and R. Nash, *Mar. Pollut. Bull.*, 2019, **138**, 145–147.
2 R. C. Thompson, Y. Olsen, R. P. Mitchell, A. Davis, S. J. Rowland, A. W. G. John, D. McGonigle and A. E. Russell, *Science*, 2004, **304**, 838.

3 A. I. Osman, M. Hosny, A. S. Eltaweil, S. Omar, A. M. Elgarahy, M. Farghali, P.-S. Yap, Y.-S. Wu, S. Nagandran, K. Batumalaie, S. C. B. Gopinath, O. D. John, M. Sekar, T. Saikia, P. Karunanithi, M. H. M. Hatta and K. A. Akinyede, *Environ. Chem. Lett.*, 2023, **21**, 2129–2169.
4 A. A. Koelmans, P. E. Redondo-Hasselerharm, N. H. M. Nor, V. N. de Ruijter, S. M. Mintenig and M. Kooi, *Nat. Rev. Mater.*, 2022, **7**, 138–152.
5 V. Stock, C. Laurisch, J. Franke, M. H. Dönmez, L. Voss, L. Böhmert, A. Braeuning and H. Sieg, *Toxicol. in Vitro*, 2021, **70**, 105021.
6 M. Shen, B. Song, G. Zeng, Y. Zhang, F. Teng and C. Zhou, *Chem. Eng. J.*, 2021, **405**, 126989.
7 E. Costigan, A. Collins, M. D. Hatinoglu, K. Bhagat, J. MacRae, F. Perreault and O. Apul, *J. Hazard. Mater. Adv.*, 2022, **6**, 100091.
8 W. J. Shim, S. H. Hong and S. E. Eo, *Anal. Methods*, 2017, **9**, 1384–1391.
9 F. Stock, C. Kochleus, B. Bänsch-Baltruschat, N. Brennholt and G. Reifferscheid, *TrAC, Trends Anal. Chem.*, 2019, **113**, 84–92.
10 A. B. Silva, A. S. Bastos, C. I. L. Justino, J. P. da Costa, A. C. Duarte and T. A. P. Rocha-Santos, *Anal. Chim. Acta*, 2018, **1017**, 1–19.
11 N. H. Ly, M.-K. Kim, H. Lee, C. Lee, S. J. Son, K.-D. Zoh, Y. Vasseghian and S.-W. Joo, *J. Nanostruct. Chem.*, 2022, **12**, 865–888.
12 I. Chakraborty, S. Banik, R. Biswas, T. Yamamoto, H. Noothalapati and N. Mazumder, *Int. J. Environ. Sci. Technol.*, 2023, **20**, 10435–10448.
13 Q. Chen, J. Wang, F. Yao, W. Zhang, X. Qi, X. Gao, Y. Liu, J. Wang, M. Zou and P. Liang, *Microchim. Acta*, 2023, **190**, 465.
14 L. Xie, K. Gong, Y. Liu and L. Zhang, *Environ. Sci. Technol.*, 2023, **57**, 25–43.
15 C. F. Araujo, M. M. Nolasco, A. M. P. Ribeiro and P. J. A. Ribeiro-Claro, *Water Res.*, 2018, **142**, 426–440.
16 Y. Liu, Z. Qin, G. Wang, X. Jia, J. Zhou, H. Li, Z. Li and X. Fang, *J. Hazard. Mater.*, 2025, **485**, 136943.
17 T. Wang, S. Li, R. Mu, Z. Lu, J. Su, J. Chen and J. Zhan, *Anal. Chem.*, 2024, **96**, 19545.
18 M. Zhao, F. Chen, B. Zhang, H. Liu, Z. Li, G. Li, M. Zhao and Y. Ma, *Talanta*, 2025, **284**, 127221.
19 B. Chaisrikhwun, S. Ekgasit and P. Pienpinijtham, *J. Hazard. Mater.*, 2023, **442**, 13004.
20 B. Chaisrikhwun, M. J. D. Balani, S. Ekgasit, Y. Xie, Y. Ozaki and P. Pienpinijtham, *Analyst*, 2024, **149**, 4158.
21 G. Xu, H. Cheng, R. Jones, Y. Feng, K. Gong, K. Li, X. Fang, M. A. Tahir, V. K. Valev and L. Zhang, *Environ. Sci. Technol.*, 2020, **54**, 15594–15603.
22 N. Jin, Y. Song, R. Ma, J. Li, G. Li and D. Zhang, *Anal. Chim. Acta*, 2022, **1197**, 339519.
23 J. Shan, Y. Zhang, J. Wang, T. Ren, M. Jin and X. Wang, *J. Hazard. Mater.*, 2020, **400**, 123202.
24 J. Y. Kim, E. H. Koh, J.-Y. Yang, C. Mun, S. Lee, H. Lee, J. Kim, S.-G. Park, M. Kang, D.-H. Kim and H. S. Jung, *Adv. Funct. Mater.*, 2024, **34**, 2307584.
25 J. Heo, J. Kim, J. Lee, H. Lee, D.-W. Shin, S. Lee, C.-H. Chung, H.-K. Na and J.-S. Wi, *Spectrosc. Lett.*, 2024, **57**, 658–665.
26 O. Guselnikova, A. Trelin, Y. Kang, P. Postnikov, M. Kobashi, A. Suzuki, L. K. Shrestha, J. Henzie and Y. Yamauchi, *Nat. Commun.*, 2024, **15**, 4351.
27 J. Guo, X. Zhang, J. Tian, W. Zhu, J. Song and H. Xiao, *Int. J. Biol. Macromol.*, 2021, **193**, 1209–1214.
28 I. Niskanen, K. Zhang, M. Karzarjeddi, H. Liimatainen, S. Shibata, N. Hagen, R. Heikkilä, H. Yoda and Y. Otani, *J. Polym. Res.*, 2022, **29**, 187.
29 S. Schiavi, M. Parmigiani, P. Galinetto, B. Albini, A. Taglietti and G. Dacarro, *Appl. Sci.*, 2023, **13**, 9291.
30 J. H. Wiley and R. H. Atalla, *Carbohydr. Res.*, 1987, **160**, 113–129.
31 Y. Luo, W. Su, M. F. Rabbi, Q. Wan, D. Xu, Z. Wang, S. Liu, X. Xu and J. Wu, *Sci. Total Environ.*, 2024, **926**, 171925.
32 X. Guo, S. Li, T. Wang, J. Su, Y. Liu, J. Chen and J. Zhan, *J. Hazard. Mater.*, 2025, **494**, 138488.